

DETECTING CHLORITE IN THE CHINESE LOESS SEQUENCE BY DIFFUSE REFLECTANCE SPECTROSCOPY

JUNFENG JI^{1,*}, LIANG ZHAO¹, WILLIAM BALSAM², JUN CHEN¹, TAO WU¹ AND LIANWEN LIU¹

¹ State Key Laboratory of Mineral Deposit Research, Institute of Surficial Geochemistry, Department of Earth Sciences,
Nanjing University, Nanjing 210093, China

² Department of Earth and Environmental Science, University of Texas at Arlington, Arlington, TX 76019, USA

Abstract—Chlorite is one of the most common Fe-bearing minerals and is susceptible to weathering in loess and soils. The conventional method for analyzing chlorite, based on XRD with the Rietveld technique, is quantitative, but very time consuming and expensive. In this paper we develop a new methodology based on diffuse reflectance spectroscopy (DRS) and selective chemical extractions to identify chlorite qualitatively in the Chinese loess sequence and present evidence suggesting that DRS may be used to quantify chlorite content. The spectral signature of chlorite in loess is obscured by Fe oxides, but becomes obvious when they are removed. Changes in the ferrous absorption band near 1140 nm vary consistently with changing chlorite content. Using this spectral feature, DRS can distinguish chlorite contents as small as 1 wt.% in loess sediments. Future possibilities for this method in other soil and sediment types need to be explored.

Key Words—China, Chlorite, Diffuse Reflectance Spectroscopy, Loess.

INTRODUCTION

Chlorite is one of the most common Fe-bearing minerals in loess sediments and soils and is very susceptible to chemical weathering. Weathering of silicate minerals is a key process in the evolution of the Earth's surface; it influences climate change (Raymo and Ruddiman, 1992; Berner, 1995) and is very important in loess and soils because such reactions ultimately control secondary mineral formation and soil development. The weathering of chlorite also influences soil-buffering capacities and acidic deposition in watersheds (Bain *et al.*, 1990), and controls the geochemical cycling of Fe, C and many inorganic nutrients that are important in soil fertility and marine bio-production (Proust *et al.*, 1986; White, 1995).

The identification and quantification of chlorite in loess and soil are conventionally based on X-ray diffraction (XRD) analysis (Bain, 1977; Proust *et al.*, 1986; Moore and Reynolds, 1997). However, because loess and soil are complex mixtures of many mineral and non-mineral components, the quantification of chlorite is difficult, and at best semi-quantitative with traditional XRD methods. These difficulties include not only the overlap of XRD peaks of other common minerals, *e.g.* kaolinite and vermiculite, and the fact that chlorite is variable in composition and structurally complex, but also the matrix effect, *i.e.* changing peak heights with varying matrix compositions. To overcome these diffi-

culties, the Rietveld technique is used for quantitative XRD analysis. With this method the scale factors of calculated XRD patterns per phase are refined until the best representation of the full experimental pattern is obtained. It is a powerful method for determining the quantities of crystalline and X-ray amorphous components in multiphase mixtures. But, because the computation needs reliable structural and chemical data for each phase in a sample, it is very time consuming and expensive, and therefore not applicable to large numbers of samples.

In this paper we suggest that a new methodology based on diffuse reflectance spectroscopy (DRS) may be useful in identifying and eventually quantifying chlorite in the Chinese loess sequence, the most complete terrestrial record of Quaternary and late Tertiary sedimentation known (Liu, 1985). Reflectance spectrophotometry has been used in remote sensing to identify a variety of minerals including olivine and pyroxene (Pieters *et al.*, 1996). It has also been suggested that remote sensing could be used to identify chlorite (King and Clark, 1989), but overlapping spectral absorption bands, especially from calcite and epidote (Dalton *et al.*, 2004) has hindered its identification by remote means. Diffuse reflectance spectroscopy of solid or ground samples has been used to identify chlorite and other minerals and is especially useful for poorly crystalline and X-ray amorphous materials that are difficult to identify with XRD. Diffuse reflectance spectroscopy appears especially sensitive to Fe-bearing minerals, notably hematite and goethite, in soils and sediments (Deaton and Balsam, 1991; Scheinost *et al.*, 1998; Ji *et al.*, 2002) where concentrations of as little as 0.01% by weight can be detected. In addition, Balsam and Damuth

* E-mail address of corresponding author:
jijunfeng@nju.edu.cn
DOI: 10.1346/CCMN.2006.0540211

(2000) indicated that chlorite has a unique NUV (near-ultraviolet, 300–400 nm)/VIS (visible, 400–700 nm)/NIR (near-infrared, 400–2500 nm) spectral signature in marine sediments. Here, we extend these observations by examining DRS spectra of chlorite in loess and paleosols and explore the possibility of a more precise quantification of chlorite at the low concentrations typical of soils and sediments.

SAMPLES AND METHODS

In this study we utilized typical loess and paleosol samples from well known loess sections at Luochuan (35.8°N, 109.4°E), Xifeng (35.4°N, 107.3°E), Lingtai (35.0°N, 107.5°E) and Baoji (34.20°N, 107.00°E). Our analyses of these loess sections concentrated on the Malan loess (L1), and the last interglacial paleosol (S1). The reference mineral ripidolite is from Flagstaff Hill, El Dorado, California (sample CCa-2 of The Clay Minerals Society Source Clays); illite is from Fithian Illinois (API clay mineral standard #35); clinochlore is from Calaveras County, California (Wards' Natural Science Establishment). Biotite was isolated from the Weishan biotite granite, Hunan province of China. Hornblende and chamosite were obtained by the Mineral Collection Laboratory of Nanjing University from Canada and Germany, respectively.

Our analysis of chlorite in loess and paleosols required the examination of both bulk and treated samples. Treatment to remove Fe oxides was necessary because these minerals have the potential to conceal the spectral signature of chlorite. This treatment involved the use of 0.5 M acetic acid to dissolve the carbonates in samples. Then we used the citrate-bicarbonate-dithionite (CBD) method (Mehra and Jackson, 1960) to eliminate the free Fe oxides. Samples were extracted twice with Na dithionite in a hot (75°C) Na citrate and Na bicarbonate solution to ensure complete removal of pedogenic Fe oxides. Microslides for DRS analysis and chlorite identification were prepared from the deferrated samples.

Diffuse reflectance spectra of samples were analyzed using a Perkin-Elmer Lambda 900 spectrophotometer with a 150 mm reflectance sphere from 400 to 2500 nm. Sample preparation and analysis followed the procedures described by Balsam and Deaton (1991). Samples were ground to <38 µm with a mortar and pestle, made into a thick slurry on a glass microslide with distilled water, smoothed and dried slowly at low temperature (<40°C). The data are written directly to a computer disk at 2 nm intervals as percent reflectance relative to the Spectralon standard.

The XRD patterns of the samples studied were obtained using a Rigaku D/max-rA diffractometer with CuK α radiation, a voltage of 40 kV, and an intensity of 25 mA. Chemical analyses of chlorite in loess samples were carried out with JEOL JXA8800M electron micro-

probe, and chemical composition of the loess samples and the reference mineral ripidolite were determined with an ARL9800 XP+ XRF (X-ray fluorescence spectroscopy) at Nanjing University.

RESULTS AND DISCUSSION

Mineral composition of the Chinese loess

Common minerals in the Chinese loess include quartz, feldspars, mica, calcite, chlorite, Fe oxide minerals (goethite, hematite, magnetite and maghemite) and clay minerals. The XRD patterns of the CBD-treated loess and paleosol samples are illustrated in Figure 1 and show strong reflections attributed to quartz, feldspar, muscovite and chlorite. These four minerals account for >80% of the total (Zheng *et al.*, 1994). In addition, the strongest reflection, 110, of hornblende is clearly seen in both loess and paleosol samples (Figure 1). The XRD patterns for the loess and paleosol samples were very similar except that there was more chlorite in the loess than in the paleosol (Figure 1). The clay fractions of loess and paleosol are dominated by illite, but also contain chlorite, kaolinite, smectite and vermiculite (Ji *et al.*, 2002).

Chlorite refers to a large family of minerals with varying chemical compositions (Klein and Hurlbut, 1993) and is present in both clay and sand fractions. Clinochlore and chamosite are its Mg-rich and Fe-rich end-members, respectively; ripidolite composition varies between them but with high Fe content, and they are all trioctahedral species. To determine the chemical composition of chlorite in Chinese loess, samples from the upper Luochuan section (L1, loess from the last glacial age) were analyzed by electron microprobe and the results are given in Table 1. The high Fe concentration of the chlorite in the loess indicates that ripidolite, a high-Fe chlorite, predominates. High-Fe and Fe-rich chlorites are easily dissolved in hot hydrochloric acid (HCl) (Moore and Reynolds, 1997). The HCl-treated, post-CBD samples show a significant decrease of chlorite reflections in XRD patterns (Figure 1) and exhibit a major change of Fe and Mg – half to two thirds was lost after the treatment (Table 2). These results indicate that the hot HCl removed predominantly chlorites leaving other silicate minerals essentially unaltered. The remaining XRD reflection at 0.7 nm may come from minor Mg-rich chlorite and kaolinite (Figure 1).

DRS of loess and chlorite

The spectra of parental bulk loess and paleosol samples are characterized by distinct absorption bands at 1400, 1900 and 2200 nm (Figure 2), resulting from the presence of OH, either in soil minerals (at 1400 and 2200 nm) or in water molecules, adsorbed or bound (at 1900 nm) (Hunt and Salisbury, 1970; Clark *et al.*, 1990). In the visible region there is a significant decrease in reflectance below 700 nm due to a charge transfer

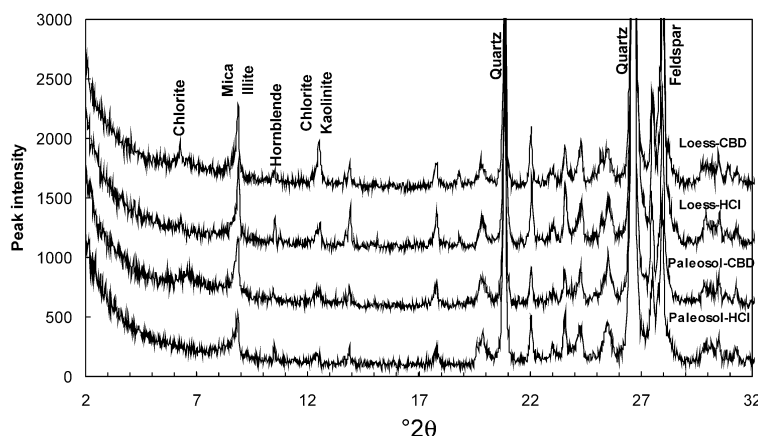


Figure 1. XRD patterns of the CBD-treated and its HCl-treated residue of typical loess and paleosol samples from the Baoji section.

absorption of Fe. Additional absorption bands are centered near 900 nm due to Fe^{3+} (Hunt and Salisbury, 1970; Clark *et al.*, 1990). Our previous studies (Chen *et al.*, 2002) showed that fine-grained, CBD-extractable, Fe oxide minerals are the dominant factor controlling reflectance changes of loess and paleosol samples, whereas organic matter, because of its generally low concentration, has only a minor influence on spectral reflectance of loess and paleosol. For soils having a small organic matter content, Fe oxides are the most important pigmenting agents (Torrent *et al.*, 1983). Hence, the removal of fine-grained, pedogenic Fe oxide from the selected samples gives rise to significant changes in spectral reflectance (Figure 2).

After CBD treatment, the spectral reflectance intensity of both the treated loess and paleosol samples increased compared to their precursors. All the treated samples display very similar reflectance spectra (Figure 2) which contain features similar to the Fe^{2+} -bearing silicates chlorite, illite and hornblende (Hunt and Salisbury, 1970; King and Clark, 1989; Clark *et al.*, 1990). The reflectance spectrum is characterized by (1) a falloff at wavelengths in the visible range; (2) absorption

bands centered near 700 nm due to charge transfer in $\text{Fe}^{2+}-\text{Fe}^{3+}$ chromophor and 900 nm due to Fe^{3+} in six-fold coordination; (3) a broad band near 1140 nm due to the Fe^{2+} in six-fold coordination; and (4) multiple complex absorption features centered near 2300 nm (Figure 3). After treatment with hot HCl, these absorption features disappeared, demonstrating that they are produced by chlorite and not from illite and hornblende because neither of them was decomposed by this treatment and both exhibited enrichment in the residuals after the treatment (Figure 1).

In fact, Fe^{2+} -bearing silicates exhibit absorption features that allow them to be distinguished from each other (Figure 3), *e.g.* in the spectral region between 800 and 1400 nm, dark mica (biotite) and illite exhibit the broad Fe^{2+} absorption feature whereas hornblende produces two absorptions similar to chlorite but centered at 930 nm (Fe^{3+} absorption) and 1180 nm (Fe^{2+} absorption); chlorite (ripidolite) has absorption features at 930 nm and 1140 nm. The CBD-treated loess samples all exhibit the same absorption features, two distinct absorptions centered at 930 nm and 1140 nm, which are indicative of chlorite (Figure 3).

Table 1. Chemical compositions (wt.%) of the chlorite in the Chinese loess (L1 loess from Luochuan section) by microprobe analysis, and in the ripidolite, by XRF.

	Range	Average	Ripidolite
SiO_2	24.47–29.68	27.28	27.25
Al_2O_3	13.62–23.72	19.77	19.74
TiO_2	0.03–2.11	0.21	0.89
Fe_2O_3	8.46–35.94	26.12	25.30
MgO	6.75–25.26	13.07	18.34
MnO	0.06–0.72	0.33	0.09
CaO	0.10–1.46	0.39	0.10
Na_2O	0.02–0.48	0.12	0.00
K_2O	0.03–0.91	0.30	0.01
$\text{Fe}_2\text{O}_3 + \text{MgO}$	30.24–44.55	39.20	43.64
Σ		84.99	91.72+9.55 (LOI)

LOI: loss on ignition

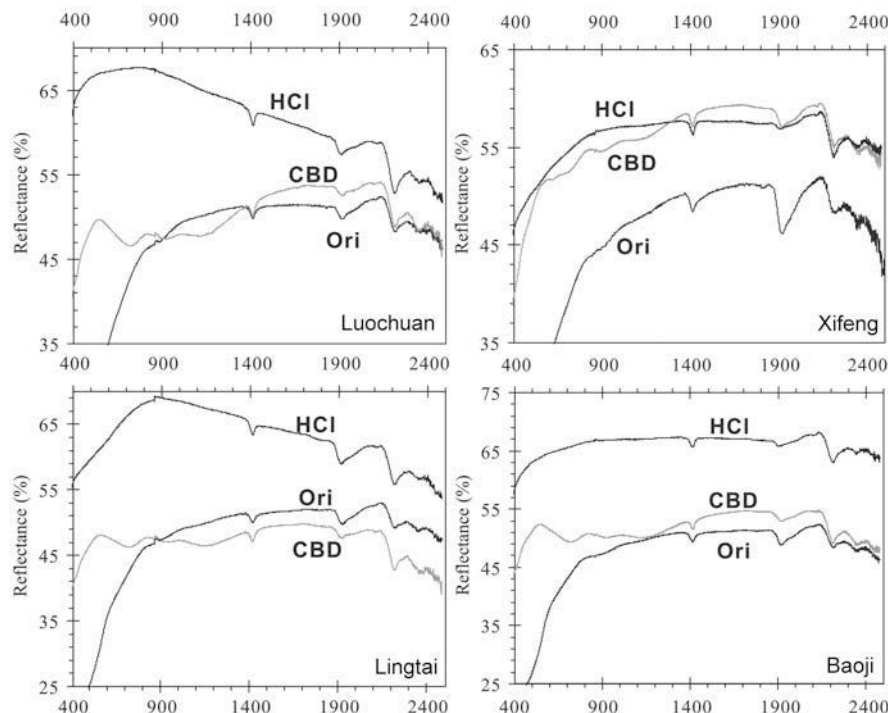


Figure 2. Diffuse reflectance spectra of the original loess (Ori) and the same CBD-treated sample (CBD) from Luochuan, Xifeng, Lingtai and Baoji. The HCl-treated residues of the deferrated samples (HCl) are shown for comparison.

Another method for analyzing reflectance spectra is to examine changes in the slope, *i.e.* the first derivative of the reflectance curves. Chlorite can be identified by its characteristic first-derivative peaks (Balsam and Damuth, 2000). For high-Fe chlorite, *e.g.* ripidolite, characteristic first-derivative peaks occur at 315 nm,

355, 425, 475 and 755–785 nm and are significantly different from those for biotite, illite and hornblende (Figure 4). Many of these peaks are clearly visible on first-derivative curves from CBD-treated loess samples (Figure 4) revealing the presence of chlorite. Prior to CBD treatment, the Fe oxides concealed the chlorite

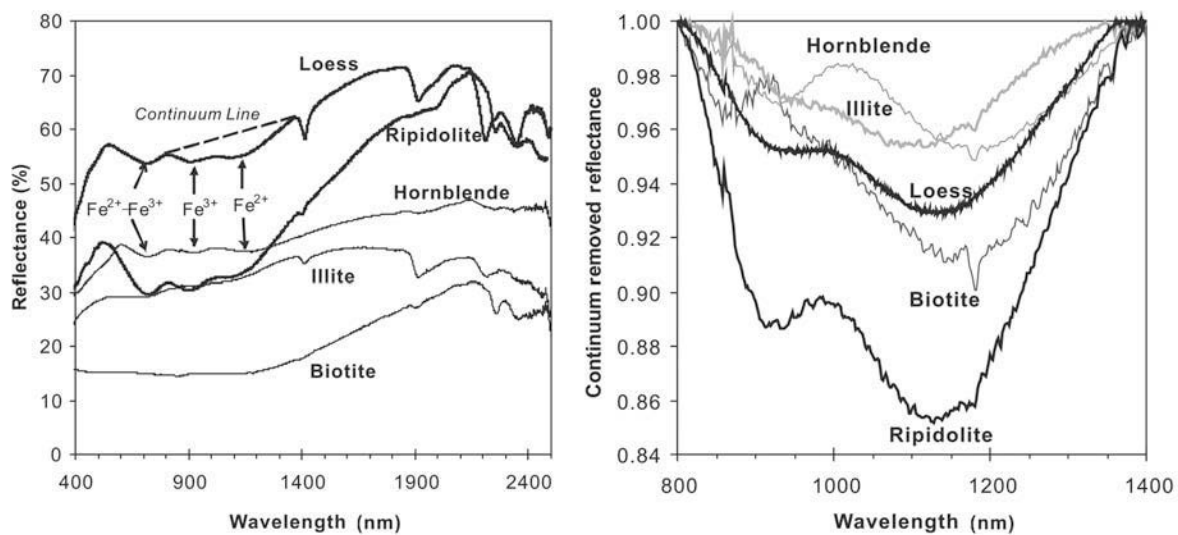


Figure 3. Diffuse reflectance spectra (left) and continuum-removed reflectance spectra (right) of the Fe²⁺-bearing silicate minerals ripidolite, hornblende, illite and biotite. The typical CBD-treated loess sample is shown for comparison. The continuum-removal approach was to fit a straight line to the reflectance continuum using two continuum tie points on either side of the absorption feature (Clark and Roush, 1984).

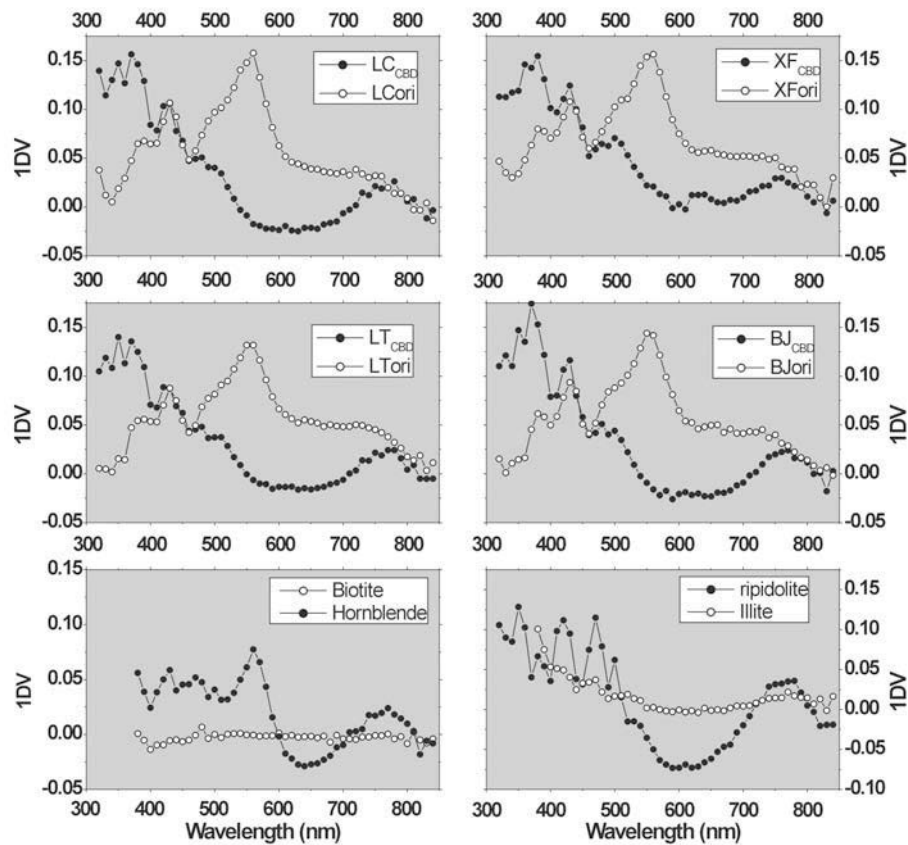


Figure 4. First-derivative curves (1DV, percent per nm) from several loess sections (LT = Lingtai, LC = Luochuan, XF = Xifeng, BJ = Baoji) and comparison with different Fe^{2+} -bearing silicate minerals: biotite, hornblende, illite and ripidolite. After CBD treatment, note the presence of first-derivative peaks similar to those of ripidolite.

peaks, with the possible exception of the peaks in the NUV.

High-resolution plots of chlorite in the 2300 nm spectral region show two diagnostic absorption features for its different species, clinochlore, ripidolite and chamosite (Figure 5). All these trioctahedral chlorites display a narrow absorption band at 2260 nm attributed to Fe-OH bands. The width of this 2260 nm band increases from clinochlore through ripidolite to chamosite, as expected, because there is an increasing FeO content. In addition, each type of chlorite exhibits a strong absorption band around 2340 nm; clinochlore at 2330 nm, ripidolite at 2342 nm and chamosite at 2364 nm. The CBD-treated loess sample clearly shows two absorptions at 2260 nm and 2354 nm (Figure 5), further confirming the identification of chlorite in loess samples with DRS.

Limits of resolution of chlorite identification with DRS

Experiments with varying concentrations of chlorite in a matrix that approximates the Chinese loess demonstrates that the chlorite can be identified to a weight concentration as low as 1% by DRS. To test correlations of spectral features with varying chlorite concentrations, a reflec-

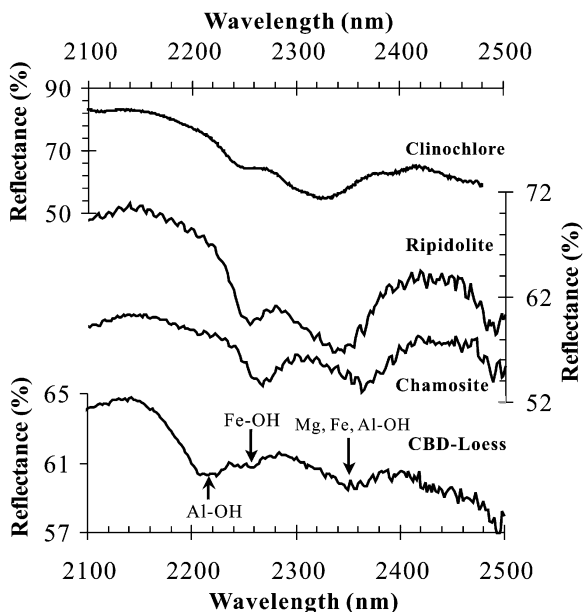


Figure 5. High-resolution spectral details of a CBD-treated loess sample compared to chlorites in the 2100–2500 nm spectral region. After CBD treatment the loess sample shows detectable chlorite absorption bands, which are indicated by the downward arrows.

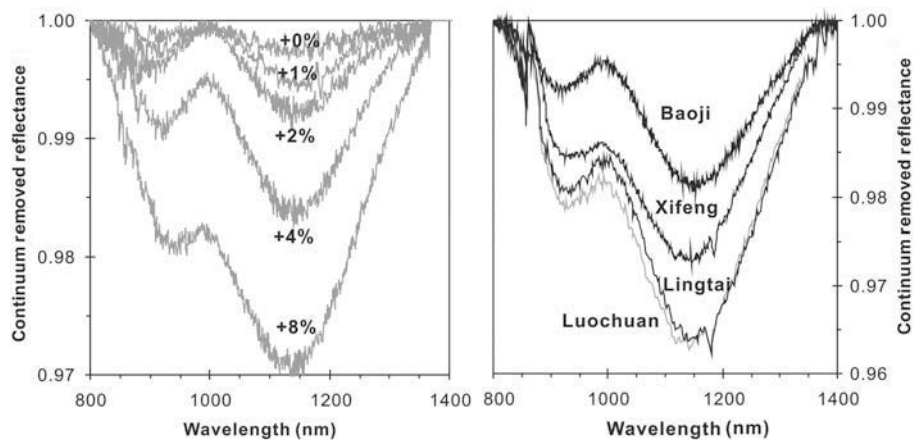


Figure 6. (Left) A series of curves illustrating how the continuum-removed reflectance spectra changes with varying concentrations of chlorite. In order to make these samples, ripidolite was mixed with deferrated L1 loess from the Xifeng section that had been treated with hot HCl. (Right) The continuum-removed reflectance spectra of the CBD-treated samples from the Luochuan, Xifeng, Lingtai and Baoji loess sections.

tance continuum was removed from the NIR spectra. That is, a line is fitted to the spectrum at two points, and the

spectrum is divided by the line, providing the normalized spectrum and band depth for the region of interest (Clark

Table 2. Comparison of the chemical composition of CBD-treated samples after hot HCl treatment. The data set includes samples from the Xifeng, Lingtai and Luochuan sections and from the original samples from the Baoji section.

Section (Number of samples)	Xifeng (8)	Lingtai (4)	Luochuan (4)	Baoji (8)
SiO ₂	HCl	75.66	76.46	76.12
	CBD	70.92	67.08	69.79
TiO ₂	HCl	0.75	0.82	0.80
	CBD	0.75	0.85	0.79
Al ₂ O ₃	HCl	12.70	12.03	12.22
	CBD	13.92	15.54	15.04
Fe ₂ O ₃	HCl	1.62	1.14	1.24
	CBD	3.40	3.58	3.55
MgO	HCl	0.98	0.74	0.82
	CBD	2.05	2.33	2.44
MnO	HCl	0.03	0.02	0.02
	CBD	0.04	0.04	0.04
CaO	HCl	0.91	0.89	0.92
	CBD	0.95	0.76	0.85
Na ₂ O	HCl	2.23	2.35	2.37
	CBD	2.19	2.32	2.31
K ₂ O	HCl	2.52	2.68	2.67
	CBD	2.61	3.33	3.06
P ₂ O ₅	HCl	0.03	0.02	0.02
	CBD	0.09	0.07	0.09
LOI	HCl	2.62	2.32	2.51
	CBD	3.01	3.60	3.41
Σ	HCl	100.05	99.60	99.84
	CBD	99.94	99.89	99.75

HCl: treated with hot HCl; CBD: treated with CBD; ORI: original samples; LOI: loss on ignition

and Roush, 1984). We found that the measured depth/strength of the ferrous absorption band near 1140 nm in the range from 800 to 1400 nm is clearly related to the abundance of chlorite. Band depth increases with increasing chlorite concentration (Figure 6) and produced a regression equation as follows:

$$\text{Chlorite (\%)} = -273 (\text{band-depth}_{1140 \text{ nm}} - 1)$$

The continuum-removed reflectance spectra of the CBD-treated samples from the Luochuan, Xifeng, Lingtai and Baoji loess sections are shown for comparison in Figure 6, and yield a range of chlorite concentrations from 7 to 10% according to the regression equation. Chlorite is the main Fe- and Mg-bearing mineral in loess. The removal of chlorite produced a significant change in the total FeO and MgO contents of the treated samples and accounted for one third of Fe₂O₃ and half of the MgO of the total samples (Table 2). Therefore, the difference in FeO and MgO contents before and after chlorite extraction should depend primarily on chlorite concentration and can be used as an estimate for the relative abundance of chlorite. According to the microprobe analysis, the total Fe₂O₃ and MgO of chlorite in the loess ranges from 30.24 to 44.55% with an average of 39.20% (Table 1). If all the acid-extracted Fe₂O₃ and MgO comes from chlorite, the 2.85–4.03% difference in Fe₂O₃ and MgO of samples from the Xifeng, Luochuan and Lingtai sections, corresponds to 7.3–10.3% chlorite, which is very similar to the spectral estimates and suggests that the spectral estimates are realistic.

The above results demonstrate the possibility of quantifying chlorite variations in loess sections with a proper reference mineral. Further research on the suitability of this method for different soil and sediment types is required and will face challenges from contaminants of other Fe-bearing silicate minerals and chemical heterogeneities of chlorite studied.

CONCLUSIONS

The results of this study demonstrate that chlorite in loess and soil can be successfully detected by DRS. The spectral signature of chlorite may be obscured by Fe oxides in the loess. When Fe oxides are removed by CBD treatment, the chlorite signature becomes obvious and can be removed with hot HCl extraction. Experiments, adding known quantities of chlorite back into the loess from which Fe oxides and chlorite had been removed, indicate that DRS can detect chlorite in this matrix at concentrations as low as 1 wt%. Changes in the ferrous absorption band near 1140 nm appear to vary consistently as the chlorite content changes and may be appropriate for quantifying the amount of chlorite in loess samples. This study opens a new approach for the identification and possible quantification of chlorite in soils and sediments.

ACKNOWLEDGMENTS

This study was funded by the National Natural Science Foundation of China through grants 40273002 and 40331001, and benefited greatly from constructive reviews by Tomas Grygar, an anonymous reviewer and the editors.

REFERENCES

- Bain, D.C. (1977) The weathering of chloritic minerals in some Scottish soils. *Journal of Soil Science*, **28**, 144–164.
- Bain, D.C., Mellor, A., Wilson, M.J. and Duthie, D.M.L. (1990) Weathering in Scottish and Norwegian catchments. Pp. 223–236 in: *The Surface Waters Acidification Programme* (B.J. Mason, editor). Cambridge University Press, Cambridge, UK.
- Balsam, W.L. and Deaton B.C. (1991) Sediment dispersal in the Atlantic Ocean: Evaluation by visible light spectra, *Reviews in Aquatic Sciences*, **4**, 411–447.
- Balsam, W.L. and Damuth, J.E. (2000) Further investigations of shipboard vs. shore-based spectral data: Implications for interpreting Leg 164 sediment composition. *Ocean Drilling Program Science Volume*, **164**, 313–324.
- Berner, R.A. (1995) Chemical weathering and its effect on atmospheric CO₂ and climate. Pp. 565–583 in: *Chemical Weathering of Silicate Minerals* (A.F. White and S.L. Brantley, editors). *Reviews in Mineralogy*, **31**. Mineralogical Society of America, Washington, D.C.
- Chen, J., Ji, J.F., Balsam, W., Chen, Y., Liu, L.W. and An, Z.S. (2002) Characterization of the Chinese loess-paleosol stratigraphy by whiteness measurement. *Palaeogeography Palaeoclimatology Palaeoecology*, **183**, 287–297.
- Clark, R.N. and Roush, T.L. (1984) Reflectance spectroscopy: Quantitative analysis techniques for remote sensing applications. *Journal of Geophysical Research*, **89**, 6329–6340.
- Clark, R.N., King, T.V.V., Klejwa, M., Swayze, G.A. and Vergo, N. (1990) High spectral resolution reflectance spectroscopy of minerals. *Journal of Geophysical Research*, **95**, 12653–12680.
- Dalton, J.B., Bove, D.J., Mladinich, C.S. and Rockwell, B.W. (2004) Identification of spectrally similar materials using the USGS Tetracorder algorithm: the calcite-epidote-chlorite problem. *Remote Sensing of Environment*, **89**, 455–466.
- Deaton, B.C. and Balsam, W.L. (1991) Visible spectroscopy – a rapid method for determining hematite and goethite concentration in geological materials. *Journal of Sedimentary Petrology*, **61**, 628–632.
- Hunt, G.R. and Salisbury, J.W. (1970) Visible and near-infrared spectra of minerals and rocks, I. Silicate minerals. *Modern Geology*, **1**, 283–300.
- Ji, J.F., Balsam, W., Chen, J. and Liu, L.W. (2002) Rapid and quantitative measurement of hematite and goethite in the Chinese loess-paleosol sequence by diffuse reflectance spectroscopy. *Clays and Clay Minerals*, **50**, 210–218.
- King, V.V.T. and Clark, R.N. (1989) Spectral characteristics of chlorite and Mg-serpentine using high-resolution reflectance spectroscopy. *Journal of Geophysical Research*, **13**, 13997–14008.
- Klein, C. and Hurlbut, C.S. (1993) *Manual of Mineralogy*. Wiley, New York, pp. 223–236.
- Liu, T.S. (1985) *Loess and the Environment*, China Ocean Press, Beijing, 251 pp.
- Mehra, O.P. and Jackson, M.L. (1960) Iron oxide removal from soils and clays by a dithionite-citrate system buffered with sodium bicarbonate. *Clays and Clay Minerals*, **7**, 317–327.
- Moore, D.M. and Reynolds, R.C., Jr. (1997) *X-ray Diffraction and the Identification and Analysis of Clay Minerals*.

- Oxford University Press, Oxford, UK, 378 pp.
- Pieters, C.M., Mustard, J.F. and Sunshine, J.M. (1996) Quantitative mineral analyses of planetary surfaces using reflectance spectroscopy. Pp. 307–325 in: *Mineral Spectroscopy: A Tribute to Roger G. Burns* (M.D. Dyar, C. McCammon and M. Schaefer, editors). Special Publication No. 5, The Geochemical Society, Houston, Texas.
- Proust, D., Eymery, J. and Beaufort, D. (1986) Supergene vermiculitization of a magnesian chlorite: iron and magnesium removal processes. *Clays and Clay Minerals*, **34**, 572–580.
- Raymo, M.E. and Ruddiman, W.F. (1992) Tectonic forcing of late Cenozoic climate. *Nature*, **359**, 117–122.
- Scheinost, A.C., Chavernas, A., Barron, V. and Torrent, J. (1998) Use and limitation of second-derivative diffuse reflectance spectroscopy in the visible to near-infrared range to identify and quantify Fe oxide minerals in soils. *Clays and Clay Minerals*, **46**, 528–536.
- Torrent, J., Schwertmann, U., Fechter, H. and Alferez, F. (1983) Quantitative relationships between soil color and hematite content. *Soil Science*, **136**, 354–358.
- White, A.F. (1995) Chemical weathering rates of silicate minerals in soils. Pp. 407–461 in: *Chemical Weathering of Silicate Minerals* (A.F. White and S.L. Brantley, editors). Reviews in Mineralogy, **31**. Mineralogical Society of America, Washington, D.C.
- Zheng, H.H., Theng, B.K.G. and Whitton, J.S. (1994) Mineral composition of loess-paleosol samples from the Loess Plateau of China and its environmental significance. *Chinese Journal of Geochemistry*, **13**, 61–72.

(Received 29 March 2005; revised 1 December 2005;
Ms. 1033; A.E. Randall T. Cygan)